EFFECT OF BORIC ACID CONCENTRATIONS ON THE CHARACTERIZATION OF THE In_2O_3 THIN FILMS GROWTH BY SPRAYING PYROLYSIS METHOD

M. TEMİZ[a*], R. G. YILDIRIM[b], M. B. BEDİR[b], M. ÖZTAŞ[b]
[a]*Selcuk University Karapınar Aydoğanlar Vocational School, 42400-Konya/TURKEY*
[b]*Eng. Fac. Department of Engineering Physics, Gaziantep University, 27310-Gaziantep/TURKEY*

Indium oxide thin films with undoped and boron doped were produced by spray pyrolysis method at a substrate temperature of 380 °C on the glass substrate using boric acid (H_3BO_3) as the dopant source. The effects of doping concentration on the features of undoped and boron doped In_2O_3 thin films have been investigated. The XRD analyses indicate that all thin films are polycrystalline with cubic structure, which is the dominant peaks of the (222), (400), (440) and (622) reflection planes with lattice parameter, approximately 9-10 Å. As the boron enters the structure, a decrease in band gap energy occurs. This decrease continues up to 0.03 M of boron additives and tends to increase again above this value. As the boron concentration increases up to 0.03 M, the resistance value decreases and the carrier concentration and Hall mobility values increase, which caused by the scattering of carriers that are severely weakened due to increased crystal quality.

(Received March 14, 2020; Accepted July 17, 2020)

Keywords: Spray pyrolysis, Structural properties, Optical properties, Indium oxide, Boron

1. Introduction

Thin film technology, which is one of the basic and defining features of technological developments, is found in most electronic devices ranging from personal computers and hardware to human communication systems [1], [2]. From a technological point of view, indium oxide (In_2O_3) thin films are important materials. In_2O_3 is a semiconductor with a large bandgap energy of around 3.55-3.75 eV. It is also an important n-type semiconductor material with good chemical stability, good electrical conductivity and high permeability in the UV-vis region.[3], [4]. These properties are very important in many areas dealing with transparent heating elements for air craft and car windows, photovoltaic devices, transparent electrodes used on electroluminescence devices and gas sensors[5], [6]. Thin films of In_2O_3 can be prepared by a variety of techniques such as chemical vapour deposition[7], spray pyrolysis[8], evaporation of indium followed by oxidation[9] and vacuum evaporation[10]. Among these techniques, thin films are produced at low cost by spray pyrolysis technique. The precise control and growth mechanism on the optoelectronic properties of the films can only be realized when they thoroughly investigate the effect of each process parameter on the film properties. This process helps us to produce high quality conductive oxide films that will allow the development of photovoltaic solar cells.

There are many studies about doped and doped In2O3 thin film. We would like to mention a few of the works that inspire us.

Manoj et all.[11] growth highly transparent and conductive indium oxide thin films onto glass substrates by using solution of indium chloride. When the study was examined, it was found that the preferential orientation of the films was sensitive to the growth parameters. It is observed that the films growth under optimum conditions have 167 nm thickness. And it also showed $2.94x10^{-4}$ Ω-cm resistivity with better transmittance than 82% at 550 nm here.

* Corresponding author: mehmettemiz@selcuk.edu.tr

Hichou et all.[12] prepared indium oxide thin films doped with fluorine by using spraying prolysis technique. The optimum substrate temperature for these films was 450 ^{0}C and their preferential orientations were (400). The electrical resistance at this temperature is $6x10^{-3}$ Ω-cm. The films have an optical transmission in the order of 95% in the visible range. F-In_20_3 has two emission peaks in the cathodoluminescence spectra. Of these peaks, the blue indirect band gap peak at 410 nm and a red emission at 650 nm.

Pramod et all.[13] prepared undoped and Sn doped In_2O_3 thin films onto clean glass by using spraying prolysis. Looking at the x-ray diffraction characterization, it is observed that the films have a cubic structure and have an average crystalline size of 10-14 nm. UV-Vis measurements prove an increase in optical transmittance in the visible region with Sn doping. With the contribution of Sn ions, they observed an improvement in both the optical and electrical properties of the In_2O_3 thin film.

Lau et all.[14] Investigated the physical properties of indium oxide (In_2O_3) thin films with different precursor concentrations. They started their experiment by preparing different precursor concentrations of indium nitrate hydrate (In (NO_3) H_20) solution. It was then started by spin coating technique before annealing at 500 °C. To characterize indium oxide thin films, an X-ray diffractometer, an ultraviolet-visible spectroscopy, a field emission scanning electron microscope and a Hall Effect Measurement System emission were used. According to the results, the film thickness showed an increase with indium oxide molarity. They observed that the film thicknesses were between 0.3-135.1 nm and the optical transparency of the films was over 94%. Lowest resistivity, mobility and carrier concentration are 2.52 Ω-cm, 26.6 cm^2/(VS) and $4.27x10^{17}$ cm^{-3} respectively for the film growth at 0.30 M.

Beji et all.[15] investigated the optical, electrical and morphological characteristics of europium doped In_2O_3 thin films growth with spraying prolysis method. All films produced by them in this study crystallize into a cubic structure. It is noted that the preferred orientation peak along the plane (222) changes to (400) with doping. The grain size, which reaches a maximum of 140 nm for 0.3% after doping, tends to be larger. Transmission for doped films is about 70%. They have band gap value between [3.43-3.51] eV. The best physical properties for europium doped In_2O_3 thin films were obtained at a doping ratio corresponding to 0.3%.

Goswami et all.[16] deposited In_2O_3 thin films on Si substrates by using pulsed laser deposition method. They employed indium oxide pellet as target. When looking at the X-ray peaks of both the films and the pellet, it is observed that they have a preferential orientation in the (222) direction. FESEM and AFM both indicate the formation of nano-pyramidal nanostructures in a high oxygen pressure environment.

According to our research, there are no reports in the literature on the investigation of boron doped In_2O_3 thin films deposited by spray pyrolysis technique. For this reason, we have drawn our attention to the feasibility of the spray pyrolysis technique for the analysis of In_2O_3:B thin films. In this paper, In_2O_3 thin films with undoped and boron doped were developed by using spray pyrolysis method and the effect of boric acid on the structural, optical and electrical properties of these films was investigated.

The undoped and boron doped In_2O_3 thin films grown by the spraying method have a polycrystalline structure. And also, all films have a preferential orientation in the (222) plane. Compared to standard XRD patterns of In_2O_3 (JCPDS 6-416), which shows that all B atoms enter the In_2O_3 lattice, XRD patterns do not have characteristic peaks associated with apparent band impurity peaks. This behaviour indicates that stoichiometry and crystal quality of thin films increase up to 0.03 M boron concentration. It was found that the concentration of 0.03 M boron doped In_2O_3 boric acid deposited at a substrate temperature of 380^{o}C was most suitable for the deposition of high-quality boron doped In_2O_3 films and corresponding to the maximum crystal grain size value of these films. Consequently, the characteristics of In_2O_3:B thin films prepared by the spray pyrolysis process depend strongly on the boron incorporation at the films. These results show us that the main effect of boron up to 0.03 M boron concentration is an increase in the size of the crystals and a decrease in the band gap energy, dislocation density and microstrain, and in this case there is an improvement in the crystal. The microstrain (ε) and dislocation density (ρ) value shows a slowly decreasing trend up to a boron concentration of 0.03 M and then increases with higher doping levels. As the boron enters the structure, a decrease in band gap energy occurs. This

decrease continues up to 0.03 M of boron additives and tends to increase again above this value. As the boron concentration increases up to 0.03 M, the resistance value decreases and the carrier concentration and Hall mobility values increase, which results from the greatly weakened carrier scattering process due to the improvement of crystallinity.

2. Experimental studies

The initial spray solution is an important production parameter for the chemical spraying technique. The solvent, type of salt, solution concentration, pH value and other additional chemicals affect the properties of the starting spray solution. Although deionized water is often used as the solvent, solvents such as ethanol, methanol, propanol or butyl acetate are used alone or together with deionized water.

All substrates used in this study have been prepared and cleaned as follows; in the first step, glass substrate is immersed into the distilled water to clean the dust on its surface during 15 minutes. Then it is taken out from the distilled water and dried. In the second step, the substrate taken from the first cup and dried is immersed into the methyl alcohol and left there for 15 minutes to clean the oily substances on the surface of the substrate, and then it is taken out from this liquid and dried in air. In the third step, the dried substrate is immersed into the third cup filled with isopropyl alcohol and it is treated again for 15 minutes to obtain a smooth surface. Finally, the substrate is treated with the distilled water as in first step to clean all residues remaining on the surface of the substrate during the other processes. The substrate cleaning process is carried out in steps as seen in Fig. 1.

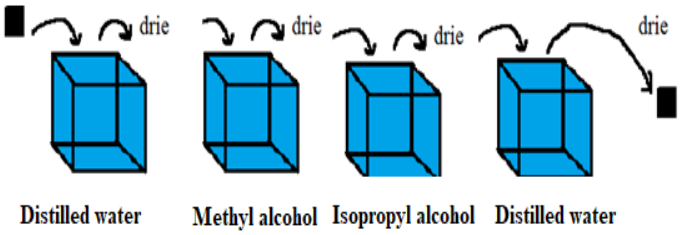

Fig. 1. The cleaning process of glass substrate.

All films were grown on cleaned glass substrates using the spray pyrolysis method at the T=380^{o}C substrate temperature. The initial solution was prepared from 0.1 M indium chloride ($InCl_2$) as an In-ion source in 50 ml of deionized water which is used as solvent. Boron-doping is achieved by adding 0.02 M, 0.03 M, 0.06 M and 0.09 M H_3BO_3 to the initial solution. The spray flow speed was set at about 0.3 ml per minute. The nozzle and substrate were kept at same position for all films. The amount of spray solution was kept constant for all films produced. Before starting production, spray solutions prepared to prevent sediment formation and to provide homogeneous mixing were mixed with magnetic stirrer for 40 minutes in the flask and then sprayed. As a result of the spraying process, the highly adherent and undoped and boron doped In_2O_3 thin film is formed on the glass substrates

The XRD pattern of In_2O_3: B thin films taken at $20<2\Theta<70$ angles by using Rigoku Miniflex X-ray Diffractometer with CuKα radiation source with a wavelength 1.54051. Energy Distributor X-Ray Analysis (EDX), known as EDS or EDAX, is an X-ray technique used to demonstrate the elemental composition or chemical characterization of an element. It is based on interactions between some X-ray excitation sources and a sample. For this purpose, Zeiss Geminisem 300 device which is within the body of high-tech application and research center of Uluğbey at University of Gaziantep was used. Absorption coefficient measurements used for 4 Jasco V 670 UV-VIS spectrophotometers for calculating the optical band gap energy E_g. It was determined by extrapolating the high absorption region of the curve to the photon energy axis[17]. The electrical resistivity values of In_2O_3: B films determined by room temperature measurements

based on four-point probe technique. Hall measurements have been also carried out employing the ‘‘Lake Shore’’ model 7604 Hall Effect measurement systems, which have been made at room temperature under a 0.5 Tesla magnetic field applied perpendicular to film surface in the Van der Pauw configuration[18]. The measurement of the Hall mobility, resistivity and charge carriers concentration were made using the Hall measurement system.

3. Results and discussions

3.1. Structural studies

X-ray diffraction patterns of undoped and boron doped In_2O_3 thin films grown at 380 ^oC substrate temperature are shown in Fig. 2. The peaks in the diffraction pattern correspond to its cubic structure, as it shows good c-axis orientation[11]. Fig. 2 shows that the undoped ad boron doped In_2O_3 thin films grown by the spraying method have a polycrystalline structure. The diffraction pattern was identified to be (222), (400), (411), (332), (431), (440) and (622) planes which is in agreement with the literature[11]. And also, all films have a preferential orientation in the (222) plane. Compared to standard XRD patterns of In_2O_3 (JCPDS 6-416), which shows that all B atoms enter the In_2O_3 lattice, XRD patterns do not have characteristic peaks associated with apparent band impurity peaks. While the density of all peaks increased up to 0.03 M boron concentration, it was observed that the density of all peaks decreased between 0.06 M to 0.09 M boron concentrations. This behaviour indicates that stoichiometry and crystal quality of thin films increase up to 0.03 M boron concentration. It was found that the concentration of 0.03 M boron doped In_2O_3 boric acid deposited at a substrate temperature of 380^oC was most suitable for the deposition of high-quality boron doped In_2O_3 films and corresponding to the maximum crystal grain size value of these films. Consequently, the characteristics of In_2O_3:B thin films prepared by the spray pyrolysis process depend strongly on the boron incorporation at the films, as similar behaviour has been observed by Bedir et al.[19]. In addition, the increase in XRD peaks shown in Fig. 1 can be said to constitute new nucleation centers of B dopant atoms. The reduction of XRD peaks at high doping levels can be explained by two factors; firstly, by the saturation of the newer nucleating centers and secondly, due to the change of the energy absorption at the time of collision, and of the physical and chemical interaction between ad-atoms and the film. It was observed that the grain size increased with increasing boron concentration up to 0.03 M, and then the crystal structure was destroyed and the grain size decreased with the increase of boron concentration. This may be due to a sufficient increase in the supply of thermal energy for recrystallization. The smaller crystallite size shows that as the barriers the carrier for transport and results in a higher grain boundary density that serves as traps for the free carrier. This trend shows that the boron dopant has created new nucleation centers to change from the homogeneous to heterogeneous nucleation type and that the crystal structure at high doping level may be disrupted.

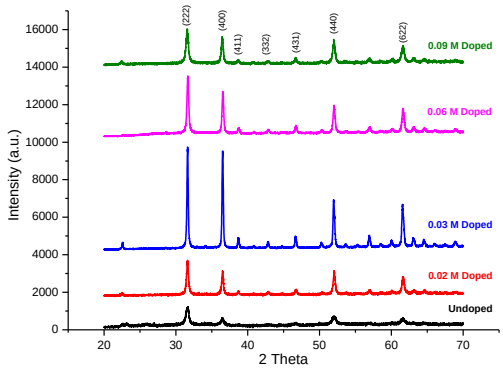

Fig. 2. X-ray diffractograms of the undoped and doped In_2O_3 thin films with different boron concentration.

The grain size of undoped and the boron doped In_2O_3 films were estimated for the (222) plane by using the Scherrer formula[20].

$$d = \frac{K\lambda}{D\cos\theta} \quad (1)$$

where D is the angular line width of the half maximum intensity, θ is the Bragg angle, λ is the X-ray wavelength and d is the grain size, K is a shape factor. Although the shape factor has a value of approximately 0.9, it shows depending on the actual shape of the crystallite. The electrical, optical and structural parameters of undoped and boron doped of In_2O_3 thin films that appear in the X-ray patterns for the peak of (222) are shown in Table 1. These results show us that the main effect of boron up to 0.03 M boron concentration is an increase in the size of the crystals and a decrease in the band gap energy, dislocation density and microstrain, and in this case there is an improvement in the crystal. The bigger crystallite size leads to a lower density of grain boundaries, which act like barriers to the transporting of the carrier and traps for the free carrier. Consequently, an increase in crystallite size can lead to a decrease in scattering at grain boundaries. These observations are linked to the results of the XRD patterns. The crystallinity of the films improves with increasing grain size, which shows a smaller number of lattice defects. It has been observed that by increasing the boron concentration, it increases the full width by half maximum (FWHM) and the crystal structure is destroyed and there is a decrease in grain size. As a result, the decrease in grain size was observed to be related to the broadening of the XRD peak. The reduction in the size of the crystal causes a higher density of grain boundaries, therefore, it carries barriers for carrier transport and creates traps for the free carrier, resulting in an increase in grain boundary scattering[21]. These results confirm the XRD patterns.

The microstrain (ε) developed in the sprayed undoped and boron doped In_2O_3 films was calculated from the equation[22],

$$\varepsilon = \frac{D\cos\theta}{4} \quad (2)$$

The dislocation density ρ is determined by the relation[22]:

$$\rho = \frac{15\varepsilon}{aD} \quad (3)$$

where D is the full width at half maximum of the (222) peak, a is the lattice constant. It can be seen from Table 1 that the microstrain (ε) and dislocation density (ρ) value shows a slowly decreasing trend up to a boron concentration of 0.03 M and then increases with higher doping levels. This reduction in microstrain and dislocation density may be owing to the dominant recrystallization process in polycrystalline films and the dispersion of interstitial In atoms through the crystallites and a decrease in the concentration of lattice defects and the occurrence of grain boundaries[23]. This observation shows that the grain size is increased, the density of dislocation and microstrain is the manifestation of the dislocation network in films, the reduction in them indicates the formation of higher quality films at the 0.03 M doping level[24].

Table 1. Variation of structural, electrical and optical parameters of the undoped and boron doped In_2O_3 thin films with different boric acid concentrations on the substrate temperature of 380 °C.

Doping Molarity (M)	2Theta (Degrees)	Miller indices (hkl)	FWHM	Thickness (μm)	Grain size (nm)	Microstrain ε x (10^{-3})	Dislocation Density x (10^{-3}) line/nm^2	Bandgap Energy (eV)	Resistivity ρ (Ω-cm) x10^3	Carrier Concentration (cm^{-3})	Mobility (cm^2/Vs)
Undoped	31.62	(222)	0.00715	5.198	23.77	2.90	1.76	3.74	33.35	2.0x10^{21}	15
0.02	31.60	(222)	0.00513	8.842	33.10	2.08	0.91	3.57	2.26	4.5x10^{21}	27
0.03	31.57	(222)	0.00363	9.260	44.36	1.47	0.50	3.51	1.28	7.4x10^{21}	39
0.06	31.61	(222)	0.00421	6.219	40.31	1.71	0.61	3.55	2.25	5.2x10^{21}	27
0.09	31.72	(222)	0.00553	4.243	30.75	2.23	1.05	3.62	4.12	3.5x10^{21}	19

3.2. Optical properties

The transmission and absorption spectra of In_2O_3: B films are given in Fig 3. In Fig. 3, undoped In_2O_3 film has highest transmittance about % 80. Although the transmittance values of the doped films were less than those of the undoped films. Transmittance values of boron doped films are observed around 75-80%. It is seen that In_2O_3:B films have low absorption in the wavelength range of 400-700 nm and the sharp increase in absorption values for all films is realized at wavelengths less than 400 nm.

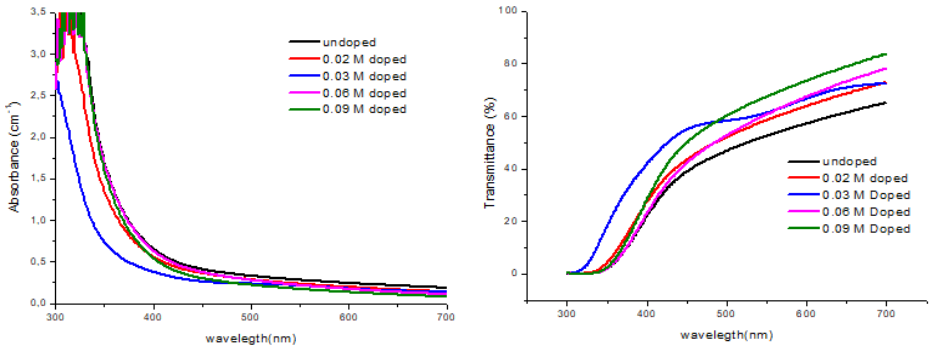

Fig. 3. Transmittance and absorbance spectrum of undoped and boron doped In_2O_3 thin films.

It gives information about the optical characterization of thin films, band gap energy and other physical properties such as band structure and optically active defects. The effect of boron concentration on the band gap values of In_2O_3 thin films was investigated. The band gap energy (E_g) was determined for all films from their reflection and transmission spectra based on Tauc equation[25].

$$\alpha h\upsilon = A(h\upsilon - E_g)^n \quad (4)$$

In the optical gap of the film, the point where the straight-line portion of the drawing obtained by drawing $(\alpha h\nu)^2 \sim h\nu$ intersects with the energy axis has given the band gap value of the films. In this way, the effect of boron concentration on band gap values of In_2O_3 thin films was

investigated and it is given in Table 1. They are of direct transition type semiconductors because $(\alpha h\nu)^2$ to hν has a linear dependence. These plots used for the optical band gap values of the films grown at 380°C substrate temperature are shown in Fig. 4. The increase in the boric acid concentration causes an increase in grain size as well as the films appear to be caused by slight decreases in the optical band gap, which can be explained by the improvement in the crystal. The band gap continues with some tail below the absorption edge shown in Fig. 4, it means that there is a high concentration of impurity states that can cause perturbation of the band structure in these films[26]. As the boric acid concentration increases up to 0.03 M, the value of the optical band gap energy decreases, resulting in the development of crystallization, which will cause the contraction band gap energy to contract due to the quantum size effect observed in semiconductor films. And donor levels degenerate and merge with the film's conduction band, which reduces bandgap. In cases where the boric acid concentration is higher than 0.03 M, it has been observed that they increase the optical band gap energy due to their lower grain sizes, scattering at grain boundaries and higher resistivity of the films. This change in band gap energy can be useful in designing a suitable window material in solar cells. From these observations, the effect of boric acid concentration on the optical band gap energy and grain size was seen. These results are are in excellent agreement with the results obtained by Bedir et al.[27] for spray deposited MnS films.

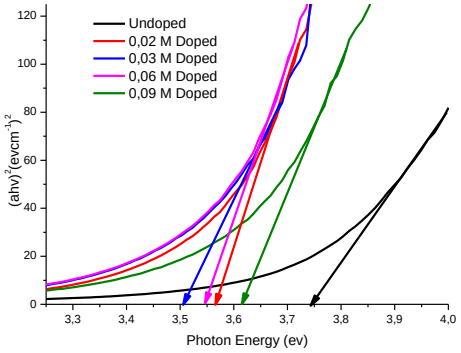

Fig. 4. Energy band-gap diagrams of undoped and boron doped In_2O_3 thin films with different boric acid concentrations.

3.3. Electrical properties

Table 1 and Fig. 5 shows the calculated values of electrical resistance, carrier concentration, and Hall mobility of the In_2O_3:B thin films. As the boron concentration increases up to 0.03 M, the resistance value decreases and the carrier concentration and Hall mobility values increase, which results from the greatly weakened carrier scattering process due to the improvement of crystallinity. Similar results were also obtained in Zr-doped In_2O_3 thin films[28]. Increasing both carrier concentration and hall mobility causes a decrease in resistance due to the increase in grain size and then narrowing of grain boundaries and donor effect of boron impurity. Increases in boron concentration of more than 0.03 M cause slight deterioration of electrical properties. Increased film resistivity is attributed to both a decrease in carrier concentration and Hall mobility. Increased electrical resistance causes grain boundary scattering and boron ions to occupy the nearest neighbouring areas more frequently, thereby preventing donor movements and causes the crystal lattice to fail. With increased boron concentration, the smaller crystallite size and higher electrical resistivity can result in increased grain boundary scatter as well as a higher grain boundary density acting as traps for carrier transport and free carrier[21]. The decrease in carrier concentration and Hall mobility may be due to decreased local donors as a result of increased oxidation of surface and resistance increase[29]. As a result, high boron concentrations cause loss of crystallinity in the films.

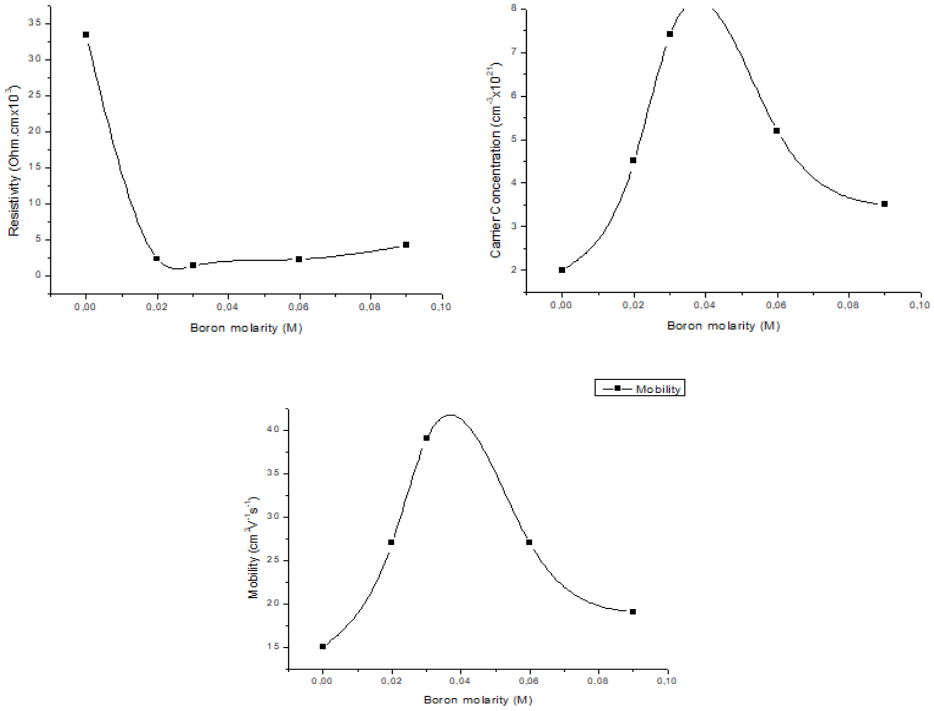

Fig. 5. The calculated values of electrical resistance, carrier concentration, and Hall mobility of the In_2O_3:B thin films.

3.4. Elemental analysis

Elemental analysis of the undoped and boron doped In_2O_3 thin films on an amorphous glass substrate at different concentration boric acid was performed using energy dispersive X-ray spectroscopy (EDAX). In order to analyze the presence of In, O and B in the undoped and boron doped In_2O_3 thin films, EDAX spectra of the samples were taken. Fig. 6 shows a typical EDAX pattern for film deposited at 380°C with the boric concentration of 0.03M which contain indium, oxygen and boron. With these spectra, it has been seen that there are expected elements in solid films. And Table 2 shows the average atomic percentages of In, O and B and the thickness of the samples, which were measurement using the energy-dispersive spectroscopy technique in a scanning electron microscope. In addition, the thickness of all films grown in this study was measured using a scanning electron microscope (SEM).

Table 2. Compositional analysis of spray deposited In_2O_3:B thin films with different boric acid concentrations.

Doping Molarity (M)	Thickness (μm)	Atomic percentage		
		In	B	O
undoped	5.198	52.57	0	47.43
0.02 M	8.842	50.70	1.5	47.80
0.03 M	9.260	50.20	3.1	46.70
0.06 M	6.219	50.40	4.4	45.20
0.09 M	4.243	45.40	5.6	49.00

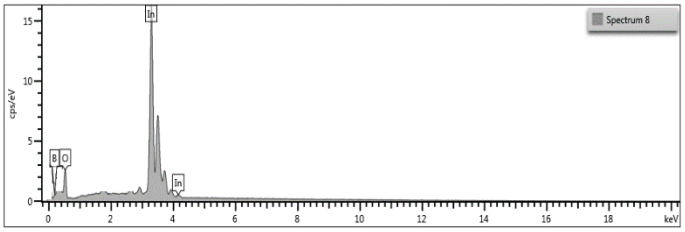

Fig. 6. EDAX spectrum of boron doped In_2O_3 thin films prepared with 0.03 M boric acid concentration.

4. Conclusions

The effect of boron doping on structural, optical and electrical properties of undoped and boron doped In_2O_3 thin films was investigated. This study showed that boric acid concentration affects the electrical, optical and structural properties of materials. The XRD pattern showed that the films were polycrystalline structure with a strong preferred orientation along (222) direction and other preferential orientation along (222), (400), (440) and (622) planes with well-defined microstructures. It is seen that the structural quality of the produced films improves up to 0.03 M boric acid concentration. If the boric acid value is high from 0.03 M level, it has been observed that the crystallization level decreases and the grain boundaries which act as defects in the structure of the films increase.

Using the optical and electrical investigations including the band gap, resistivity, carrier concentrations and Hall mobility it was determined that the band gap and resistivity of In_2O_3:B thin films decreases, while carrier concentrations and Hall mobility increase with increase of the boric acid concentrations up to 0.03 M, due to the improved crystallization of the films and the changes in grain size. Therefore, it can be said that 0.03 M boric acid incorporations are the most suitable boric acid contents, to improve the crystallinity of In_2O_3:B thin films. Due to the described properties, boron-doped indium oxide thin films can be used in many areas dealing with transparent heating elements, photovoltaic devices, transparent electrodes used in electroluminescent devices and gas sensors for aircraft and car glass.

References

[1] L. Eckertová, Physics of Thin Films, Plenum Press, Berlin: Springer, 1986.
[2] S. Sönmezoğlu, M. Koç, S. Akin, Erciyes Univ. J. Sci. Technol. **28**, 389 (2012).
[3] A. Moses Ezhil Raj et al., Phys. B Condens. Matter **403**, 544 (2008).
[4] T. Fukano, T. Motohiro, H. Hashizume, Jpn. J. Appl. Phys **44**, 12 (2005).
[5] G. Korotcenkov et al., Sensors Actuators, B Chem. **99**, 297 (2004).
[6] G. Korotcenkov et al., in Sensors and Actuators, B: Chemical **103**, 13 (2004).
[7] J. Kane, H. P. Schweizer, W. Kern, Thin Solid Films **29**, 155 (1975).
[8] J. Manifacier, L. Szepessy, J. Bresse, M. Peroten, R. Stuck, Appl. to Sol. energy conversion, part 1 - Prep. Charact. **14**, 109 (1979).
[9] S. Noguchi, H. Sakata, J. Phys. D. Appl. Phys. **13**, 1129 (1980).
[10] M. Girtan, Surf. Coatings Technol. **184**, 219 (2004).
[11] P. K. Manoj, K. G. Gopchandran, P. Koshy, V. K. Vaidyan, B. Joseph, Opt. Mater. **28**, 1405 (2006).
[12] A. El Hichou, M. Addou, M. Mansori, J. Ebothé, Sol. Energy Mater. Sol. Cells **93**, 609 (2009).
[13] N. G. Pramod, S. N. Pandey, P. P. Sahay, J. Therm. Spray Technol. **22**, 1035 (2013).
[14] L. N. Lau, N. B. Ibrahim, H. Baqiah, Appl. Surf. Sci. **345**, 355 (2015).
[15] N. Beji, M. Souli, M. Ajili, S. Azzaza, S. Alleg, N. K. Turki, Superlattices and

Microstructures **81**, 114 (2015).
[16] S. Goswami, A. K. Sharma, AIP Conf. Proc. **2082**, 3 (2019).
[17] M. Bedir, A. Tunç, M. Öztas, Acta Phys. Pol. A **129**, 1159 (2016).
[18] L. van der Pauw, Philips Res. Reports **20**, 220 (1958).
[19] M. Bedir, M. Öztaş, H. Kara, J. Mater. Sci. Mater. Electron. **499**, (2013).
[20] B. D. Cullity, Elements of X-ray diffraction, Addision-Wesley Pub. Co. Ind., London, 1967.
[21] H. Kim, J. Appl. Phys. **88**, 6021 (2000).
[22] M. Bedir, M. Öztaş, Ö. F. Bakkaloğlu, R. Ormanci, Eur. Phys. J. B **45**, 465 (2005).
[23] F. Rong, G. D. Watkins, Phys. Rev. Lett. **58**, 1486 (1987).
[24] N. Jabena Begum, K. Ravichandran, J. Phys. Chem. Solids **74**, 841 (2013).
[25] N. Beji, M. Souli, M. Reghima, S. Azzaza, S. Alleg, N. Kamoun-Turki, Mater. Sci. Semicond. Process. **56**, 20 (2016).
[26] M. Öztaş, M. BEdir, J. Appl. Phys. **2**, 214 (2001).
[27] M. Bedir, M. Öztaş, S. S. Çelik, T. Özdemir, Acta Phys. Pol. A **126**, 840 (2014).
[28] H. Kim, J. S. Horwitz, G. P. Kushto, S. B. Qadri, Z. H. Kafafi, D. B. Chrisey, Appl. Phys. Lett. **78**, 1050 (2001).
[29] Q. B. Ma et al., J. Phys. D. Appl. Phys. **41**, 5 (2008).